

A hybrid model of cell cycle in mammals

Jonathan Behaegel^{*,‡}, Jean-Paul Comet^{*,§}, Gilles Bernot^{*,¶},
Emilien Cornillon^{*,||} and Franck Delaunay^{†,**}

**Université Nice-Sophia Antipolis
I3S-UMR CNRS 7271, CS 40121
06903 Sophia Antipolis Cedex, France*

*†Université Nice Sophia Antipolis
CNRS UMR7277, INSERM U1091*

*Institut de Biologie Valrose
06108 Nice, France*

‡behaegel@i3s.unice.fr

§comet@unice.fr

¶bernot@unice.fr

||ecornillon@i3s.unice.fr

***franck.delaunay@unice.fr*

Accepted 12 October 2015

Published 24 December 2015

Time plays an essential role in many biological systems, especially in cell cycle. Many models of biological systems rely on differential equations, but parameter identification is an obstacle to use differential frameworks. In this paper, we present a new hybrid modeling framework that extends René Thomas' discrete modeling. The core idea is to associate with each qualitative state "celerities" allowing us to compute the time spent in each state. This hybrid framework is illustrated by building a 5-variable model of the mammalian cell cycle. Its parameters are determined by applying formal methods on the underlying discrete model and by constraining parameters using timing observations on the cell cycle. This first hybrid model presents the most important known behaviors of the cell cycle, including quiescent phase and endoreplication.

Keywords: Discrete modeling; hybrid modeling; mammalian cell cycle.

1. Introduction

Regulatory networks are models based on graphs which we use to obtain a simpler view of gene regulation. Gene regulation is then the process of turning genes on and off and is made possible by a network of interactions using regulatory proteins. Gene regulation guarantees that appropriate genes are expressed at proper times specially during early development where cells begin their specific functions. Gene regulation also helps an organism to respond to its environment.

The various existing modeling frameworks differ by the aspects they highlight. Stochastic models emphasize non-determinism, differential models represent a system with a lot of details (transcription, traduction, transports, etc.) and give precise trajectories in terms of concentrations, qualitative models focus on the major features that explain the observations (only main causalities are taken into account), and hybrid models link qualitative aspects with continuous variables such as time. For gene networks, the qualitative framework by Thomas^{1,2} has become a standard because it highlights the qualitative nature of gene regulations and powerful software platforms have been designed that help the biologists in designing and analyzing models. Unfortunately, the qualitative nature of discrete models leads to completely abstract time scale: When chronometrical time plays a crucial role in the biological system, Thomas' discrete method is not sufficient.

Whatever the modeling framework, the main difficulty relies on the identification of *good* parameter values. For differential, probabilistic, discrete or hybrid models, parameters pilot the dynamics, and finding accurate values remains a difficult step. For discrete modeling frameworks like the one of Thomas, *formal methods* assist the modeler to automatically select or constrain the parameters in order to get accurate dynamics.^{3,4} When the models have to handle durations, they can be described in terms of differential systems or in terms of hybrid models. Whereas parameter identification in differential systems is a hard problem even when the nature of differential systems is well known, hybrid modeling frameworks can still be assisted by computer-aided methods to help the modeler to setup the parameters.

In the context of gene networks, several hybrid frameworks have been designed in order to take into account timing informations.⁵⁻⁷ In this paper, we introduce a new hybrid modeling framework where the discrete kinetic parameters of Thomas's approach are extended into "celerities" (real number values), allowing us to deduce the time spent in each discrete state. To illustrate the ability of this hybrid modeling framework to represent timing information, we model the well-studied *cell cycle*, that gives several daughter cells starting from a parent cell. In this paper, we focus on mitosis which produces two daughter cells.

The behavior of the cell cycle in mammals can be summed up as follows. Cell cycle displays four phases which are always linked in the same order: G1, S, G2, and M. Each of these phases is controlled by a protein complex made of a Cyclin and a Cdk (Cyclin-dependent kinase). For example, Cyclin A/Cdk2 governs the S phase of cell cycle. Checkpoints exist for G1/S and G2/M transitions. They allow the cell to control that DNA is not damaged before continuing cell cycle and the second checkpoint additionally controls that DNA is properly replicated before starting mitosis (M phase). At the end of mitosis, that is after cell division, progeny cell can stop cell cycle in order to remain in an idle state G0 called *quiescent phase*. This phase terminates when the cell starts a new cell cycle. In another particular case of the cell cycle, the endoreplication allows the cell to terminate earlier the classical behavior by stopping the cell cycle at the first step of mitosis (no cellular division): Cell starts mitosis (prophase step) but it is stopped just before cell division. The cell

directly goes towards the middle or end of the G1 phase without leading to the development of two daughter cells. Therefore, the parent cell grows and its genome doubles: This phenomenon leads to polyploidy.

In this paper, we use biological knowledge on the cell cycle in order to constrain the parameters of our hybrid model. Because the hybrid model relies on a discrete one, we determine parameters using both formal methods for discrete parameter identification and measurements of time spent in different phases.

The paper is organized as follows. We first define the hybrid modeling framework based on Thomas' discrete one (Sec. 2). Then Sec. 3 is devoted to the interaction graph of the cell cycle. Section 4 focuses on the identification of parameters of both discrete and hybrid models. Section 5 sketches the results obtained by simulations. Finally, we discuss the limits of our hybrid model of the cell cycle in Sec. 6.

2. Hybrid Modeling Framework

2.1. Thomas' discrete framework

In 1973, Thomas designed a discrete framework well suited for modeling dynamics of gene networks.^{1,2} Quantitative concentrations of gene products are abstracted into qualitative levels. This abstraction is an acceptable simplification because real concentrations are not accurately measurable *in vivo* and the thresholds between qualitative levels are chosen in a clever way.

The gene regulations are classically represented by an interaction graph where vertices abstract gene products and arrows the regulations between them. When a gene regulates several targets, there is no reason that the regulations take place exactly at the same concentration. In such a case, we must consider more than two (on/off) abstract levels to represent the set of targets regulated by the gene. These genes are said *multivalued*. The dynamics of a model is driven by kinetic parameters, that give the qualitative variations for each gene product. From these parameters, a state transition graph showing the behaviors of the system can be easily built.

Here we complete the first formalization^{3,8} of this approach using multiplexes, that specify, via a logical formula, the cooperation or concurrency between two or more regulators of the same target (see Fig. 1(a)). Vertices are called *variables* because these latter can gather genes which are co-expressed.

Definition 1. A *gene regulatory network (GRN) with multiplexes* is a tuple $N = (V, M, E, \mathcal{K})$ satisfying the following conditions:

- V and M are disjoint sets, whose elements are called *variables* and *multiplexes*, respectively.
- $G = (V \cup M, E)$ is a labeled directed graph such that:
 - (a) edges of E start from a multiplex and end to a variable.
 - (b) every variable v of V is labeled by a positive integer b_v called the *bound* of v .

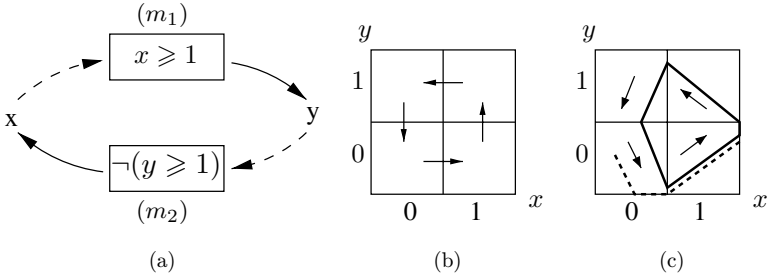


Fig. 1. (a) Graphical representation of a gene regulatory graph with multiplexes. Dashed lines represent participation of variables in multiplexes (not present in Definition 1). (b) State graph obtained with parameters $K_{x,\{\}} = 0$, $K_{x,m_2} = 1$, $K_{y,\{\}} = 0$, $K_{y,m_1} = 1$. (c) Hybrid trajectories obtained by the following celerities: $C_{x,\{\},0} = -1.5$, $C_{x,\{\},1} = -4$, $C_{x,\{m_2\},0} = 1.5$, $C_{x,\{m_2\},1} = 4$, $C_{y,\{\},0} = -3.33$, $C_{y,\{\},1} = -3$, $C_{y,\{m_1\},0} = 2.4$ and $C_{y,\{m_1\},1} = 3$.

(c) every multiplex m of M is labeled by a formula φ_m belonging to the language \mathcal{L} inductively defined by:

(i) If v belongs to V and $s \in \mathbb{N}$, then $v \geq s$ is an atom of \mathcal{L} .

(ii) If φ and ψ belong to \mathcal{L} then $\neg\varphi$, $(\varphi \wedge \psi)$ and $(\varphi \vee \psi)$ also belong to \mathcal{L} .

- $\mathcal{K} = \{K_{v,\omega}\}$ is a family of integers indexed by $v \in V$ and $\omega \subset N^-(v)$, where $N^-(v)$ is the set of predecessors of v in G (that is, the set of multiplexes m such that $m \rightarrow v$ is an edge of E). Each $K_{v,\omega}$ must satisfy $0 \leq K_{v,\omega} \leq b_v$.

Definition 2 (States, satisfaction relation and resources). Let N be a GRN and V be its set of variables. A *discrete state* of N is a function $\eta : V \rightarrow \mathbb{N}$ such that $\eta(v) \leq b_v$ for all $v \in V$. The satisfaction relation \models_N between a state η of N and a formula φ of \mathcal{L} is inductively defined by:

- If φ is an atom of the form $v \geq s$, then $\eta \models_N \varphi$ if and only if $\eta(v) \geq s$.
- If $\varphi \equiv \neg\psi$ then $\eta \models_N \varphi$ if and only if $\eta \not\models_N \psi$.
- If $\varphi \equiv \psi_1 \wedge \psi_2$ then $\eta \models_N \varphi$ if and only if $\eta \models_N \psi_1$ and $\eta \models_N \psi_2$; and we proceed similarly for other connectives.

For $v \in V$, a multiplex $m \in N^-(v)$ is a *resource* of v at state η if $\eta \models_N \varphi_m$. The *set of resources* of v at state η is defined by $\rho(\eta, v) = \{m \in N^-(v) \mid \eta \models_N \varphi_m\}$.

According to Definition 2, a resource is a multiplex whose formula is satisfied at the current state. The parameter that gives the variation of variable v is the one associated with the set of resources of v at the current state. We call *focal point* the state whose coordinates are given by the parameters associated with each variable.

Definition 3 (State Graph). Let $N = (V, M, E, \mathcal{K})$ be a GRN. The *state graph* of N is the directed graph \mathcal{S} defined as follows: The set of vertices is the set of states of N , and there exists an arc (called transition) $\eta \rightarrow \eta'$ if one of the following conditions is satisfied:

- for all variables $v \in V$ we have $\eta'(v) = K_{v,\rho(\eta,v)}$, and then $\eta' = \eta$,

- there exists $v \in V$ such that $\eta(v) \neq K_{v,\rho(\eta,v)}$, and

$$\eta'(v) = \begin{cases} \eta(v) + 1 & \text{if } \eta(v) < K_{v,\rho(\eta,v)}, \\ \eta(v) - 1 & \text{if } \eta(v) > K_{v,\rho(\eta,v)} \end{cases} \quad \text{and for all variables } u \neq v, \eta'(u) = \eta(u).$$

The first item of Definition 3 expresses a stable state: The focal point coincides with the current state. The second item expresses when it is possible to go from a state to another one: If the value of the variable v is lower (respectively greater) than the parameter value associated with v , then this variable can increase (respectively decrease) by one unit. Note that at each step, only *one* variable can evolve. The construction of the state graph is illustrated on the toy example in Fig. 1(b).

The combinatorics of acceptable parameter values is exponential (because the number of parameters associated with a variable depends on the number of possible resources). In order to decrease this combinatorics, we admit the Snoussi's condition⁹:

$$\forall v \in V, \quad \forall \omega, \omega' \subset N^-(v), \quad \text{if } \omega' \subseteq \omega, \quad \text{then } K_{v,\omega'} \leq K_{v,\omega}.$$

2.2. Hybrid modeling based on Thomas' modeling

Definition 4 introduces the *hybrid gene regulatory networks* (HGRN), a formalism using Thomas' discrete states, and adding continuous variables allowing the handling of time. The *celerities* can be viewed as abstract speeds.

Definition 4. A HGRN is a tuple $N = (V, M, E, \mathcal{C})$ where V, M, E satisfy the first two items of Definition 1 and where $\mathcal{C} = \{C_{v,\omega,n}\}$ is a family of real numbers indexed by (v, ω, n) triplets where $v \in V, \omega \subset N^-(v)$ and n is an integer such as $0 \leq n \leq b_v$.

There is a strong connexion between the discrete Thomas formalism and our hybrid formalism: The sign of the celerities can be deduced from the discrete parameters. The discrete parameters describe the focal point towards which the system is attracted, and, because the celerities express the directions of trajectories, their signs are constrained by the focal point. In Fig. 2, we represent a set of states that differ only by the value of a variable v and we assume that they share the same set of resources ω for v . Let $n = 0 \dots 3$ be the states of v . When $K_{v,\omega}$ differs from 0 or b_v ,

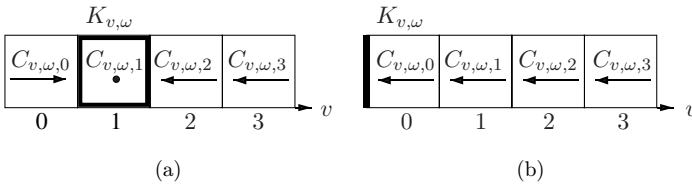


Fig. 2. Relationship between Thomas' parameters and celerities. Here, each discrete state is supposed to have the same set of resources ω for a given variable v . (a) If $K_{v,\omega} = 1$ then below this discrete level, celerities are positive, above it, they are negative (see arrows). In the state where $v = 1$, the celerity is null. (b) $K_{v,\omega}$ is supposed to be equal to 0 and the variable v is attracted towards 0: The celerity in the discrete state where $v = 0$, is negative or null.

three cases have to be considered (Fig. 2(a)): If n is below $K_{v,\omega}$, we have $C_{v,\omega,n} > 0$, if n is above $K_{v,\omega}$, we have $C_{v,\omega,n} < 0$ and if n is equal to $K_{v,\omega}$, we have $C_{v,\omega,n} = 0$ because v has already reached the value towards which the variable is attracted. If the parameter $K_{v,\omega}$ equals 0 or b_v (Fig. 2(b)), two choices can be made: One can consider as previously that, when the value of v is equal to the parameter, the variable no longer evolves ($C_{v,\omega,0} = 0$ or $C_{v,\omega,b_v} = 0$), or one can consider that the variable is attracted towards the external boundary and in this case, for all n , the signs of celerities $C_{v,\omega,n}$ are constant.

Definition 5. Let us consider a HGRN $N = (V, M, E, \mathcal{C})$. A hybrid state of N is a couple $h = (\eta, \pi)$ where:

- η is a function of V in \mathbb{N} such as $\forall v \in V, 0 \leq \eta(v) \leq b_v$; η is called the discrete state of h ,
- π is a function of V in the real interval $[0, 1]$. π is called the fractional part of h .

Here η represents the qualitative part of the current state, the fractional part reveals the exact position $(\pi(v))_{v \in V}$ inside the discrete state. For each variable $v \in V$, the set of hybrid coordinates of v $\{(\eta(v), \pi(v)) | \pi(v) \in [0, 1], \eta(v) = n\}$ can be interpreted as the real interval $[n, n + 1]$.

Definition 6. Let us consider a HGRN $N = (V, M, E, \mathcal{C})$ and a hybrid state $h = (\eta, \pi)$. The *touch delay* of v noted $\delta_h(v)$ is the time allowing v to reach the border of the current discrete state. For each $v \in V$, δ_h is the function of V in \mathbb{R}^+ defined by:

- if $C_{v,\rho(\eta,v),\eta(v)} = 0$, then $\delta_h(v) = +\infty$,
- if $C_{v,\rho(\eta,v),\eta(v)} > 0$, then $\delta_h(v) = \frac{1-\pi(v)}{C_{v,\rho(\eta,v),\eta(v)}}$,
- if $C_{v,\rho(\eta,v),\eta(v)} < 0$, then $\delta_h(v) = \frac{\pi(v)}{|C_{v,\rho(\eta,v),\eta(v)}|}$.

Definition 6 gives the times necessary for the variables to reach a border of the current discrete state. When experimental data allow us to derive the time spent in a state, the touch delay leads to constraints on celerities.

We do not formalize here the whole dynamics associated with such a hybrid model because the behavior is intuitive: Starting from a hybrid state $h = (\eta, \pi)$, the celerities define a linear evolution inside the discrete state until touching a border. At the border, several situations can appear. Let us consider that the trajectory reaches a border separating two discrete states that differ by the value of variable v .

- (1) If the second discrete state can accept trajectories from the border (celerities of v in both neighbor states have the same sign), then the trajectory goes into the second discrete state and can be extended using celerities of the second one.
- (2) If the second discrete state prevents trajectories to enter (celerities of v in both neighbor states have opposite sign), then the trajectory cannot enter the second discrete state and then slides along the border according to celerities of other variables.

If the reached border is an external one ($\eta(v) = 0$ and $C_{v,\rho(\eta,v),0} < 0$ or symmetrically $v = b_v$ and $C_{v,\rho(\eta,v),b_v} > 0$), the trajectory cannot cross the border and it slides as in the previous case.

Figure 1(c) is a representation of the hybrid trajectories of the toy example. Directional vectors represent the relative celerities in each discrete state.

3. Molecular Aspects of the Cell Cycle

3.1. Sketch of the cell cycle functioning

Cell proliferation realized by the cell cycle is essential for individual survival. It ensures tissues renewal or cell growth. Mitosis is a biological phenomenon giving rise to two daughter cells starting from a unique cell. The offspring have the same characteristics than parent cell. The cell cycle is classically divided into four phases called respectively G1, S, G2, and M, which come one after another, leading to cell division, see Fig. 3(a). Between G1 and S and between G2 and M, there exist two checkpoints: If conditions are not satisfied, the cell cycle stops and there is no cell division.

From a molecular point of view, the cell cycle is mainly controlled by complexes made of a Cyclin and a kinase of the family Cdk, ¹⁰ see Fig. 3(b):

- (1) The cell cycle starts when entering into G1 phase depending on growth factors present in the cell. During this phase, the cell prepares replication and increases its size. The growth factors stimulate the Cyclin D/Cdk4-6 complex, ensuring the activation of Cyclin E/Cdk2. This last complex allows the cell cycle to pass G1/S checkpoint¹¹ (verification of the non-damage of DNA).

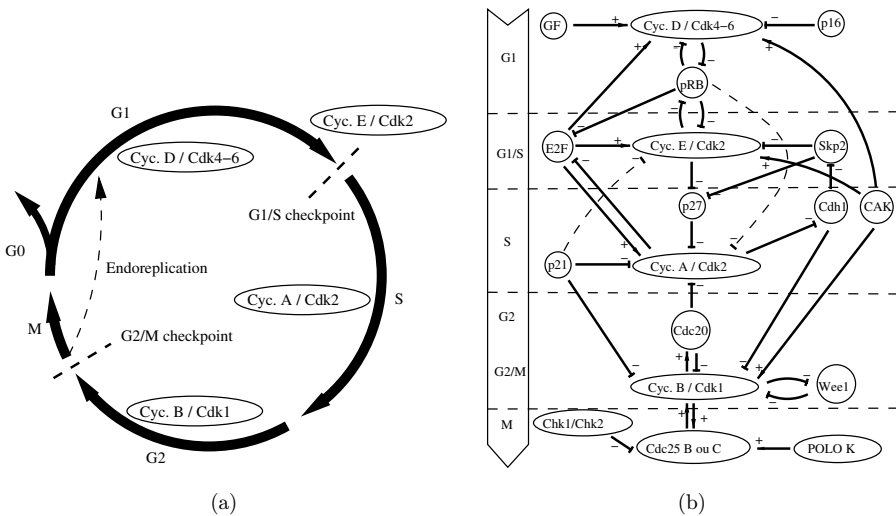


Fig. 3. (a) Cell cycle phases. (b) Molecular aspects of cell cycle.

- (2) During S phase, Cyclin A/Cdk2 is indirectly stimulated by Cyclin E/Cdk2. Then the cell continues to grow and its centrosome is replicated.
- (3) During G2 phase, cell prepares its division and achieves replication: The Cyclin A/Cdk2 activates Cyclin B/Cdk1 so that it passes through the G2/M checkpoint (verifications of non-damage of DNA and ending of replication).
- (4) The M phase represents the steps of mitosis to make two daughter cells. In particular, a surveillance mechanism exists which recognizes the kinetochores attached on mitotic spindles that activates APC protein: The latter activates proteins triggering the cleavage of sister chromatids (metaphase/anaphase transition).

All these complexes are synthesized and degraded successively during a cell cycle, but several complexes can be expressed simultaneously. These complexes are also stimulated by kinases (Cdc25 or CAK complex) and they are inhibited by CKI (Cdk Inhibitors like p21 or p27) or by kinases like Wee1. Even if the molecular interaction map of the mammalian cell cycle is well known and rather large,¹² here we focus on essential components that regulate cell cycle.

In addition to the classical cell cycle, one observes a quiescent phase called G0 that is the state when cell neither divides nor prepares division. Cells can enter G0 at the end of cell division, and then they do not proliferate. They can remain in the quiescent phase from a few hours to several years.¹³ Then cells can re-enter into a new cell cycle starting in G1 phase.

Endoreplication is also linked to cell cycle¹⁴: Cells can start mitosis without finishing it. These cells duplicate their DNA (a cell with more than two copies of its chromosomes is said *polyploid*) and their cytosols grow. In mammals, megakaryocytes making platelets in blood have 128 copies of their chromosomes.

3.2. A simplified 5-variable gene network

Our interaction graph modeling molecular aspects of cell cycle is inspired by a John Tyson's model,¹⁵ which has been designed to represent mammalian or yeast cell cycle. We add supplementary biological phenomena in order to get an interaction graph specific for mammals, in which both checkpoints and surveillance mechanism of mitosis are taken into account. In Fig. 4, the simple multiplexes (with a unique input and a unique output) are replaced by arrows labeled by a sign and a threshold. For example:

- The arrow from SK to A is labeled by +2. It codes for the multiplex with formula $(SK \geq 2)$ pointing towards A.
- The arrow from SK to En is labeled by -1. It codes for the multiplex with formula $\neg(SK \geq 1)$ pointing towards En.

Our model differs from Tyson' model by the three following aspects:

- First, we include the CAK complex (Cyclin H/Cdk7) in SK: CAK is an activator of Cyclin E/Cdk2¹⁶ whose activation is necessary to pass the G1/S checkpoint.

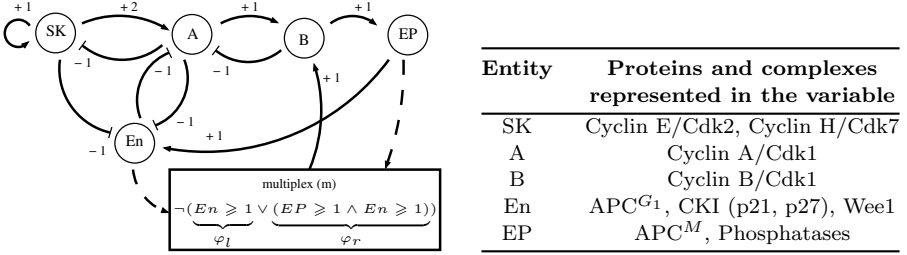


Fig. 4. A simplified 5-variable gene network of the mammalian cell cycle. APC^M is a complex involved in surveillance mechanism in order to enter into anaphase (third step of mitosis). The combined effects of the APC^{G1}, p27, and Wee1 inactivate Cdk1, Cdk2, Cdk4, and Cdk6.

Because CAK and Cyclin E/Cdk2 are both in SK, an autoregulation of SK is added. Moreover, because Cyclin E activates Cyclin A (involved in A), SK activates A. Knowing that CAK activates first Cyclin E/Cdk2 then Cyclin A/Cdk2, the level of the autoregulation of SK is lower than the level of the activation of SK on A. We chose accordingly the thresholds: The autoregulation of SK takes place at level 1 and the regulation of SK on A at level 2. Thus, SK is multivalued.

- Secondly, in the Tyson’s model, Cyclin A and Cyclin B are both represented by a unique variable. We split these cyclin complexes because they act in different phases whose durations are different.
- The last modification is the addition of the multiplex m : It describes, *via* a logical formula, the conditions under which B is inhibited by EP and En. It is well known that these variables, when simultaneously present, inhibit B¹⁷ (part φ_r of the formula). However, other biological knowledge points out that En inhibitors are sufficient¹⁸ (part φ_l of the formula). The formula of m can then be simplified: An equivalent formula is $\neg(En \geq 1)$. Thus EP could be removed from the interaction graph. Nevertheless, we decide to keep EP because the APC^M protein acts during the surveillance mechanism of mitosis¹⁹ which we want to represent.

4. Parameter Identification

4.1. Identifying discrete parameters from traces

SK is three-valued and the other variables are Boolean. The number of states is $2^4 \times 3 = 48$. In the sequel, we note “abcde” the state where SK = a , EP = b , A = c , B = d and En = e . For example, the state (SK = 0, EP = 0, A = 1, B = 0, En = 0) is denoted 00100. Thomas’ dynamics is controlled by 26 parameters (see Table 1).

We constrain the set of parameters using a “genetically modified” Hoare logic.²⁰ Classical Hoare logic for imperative programs has been introduced to prove correctness of programs. Hoare introduced the notation $\{P\}p\{Q\}$ to mean “If the

Table 1. Constraints on discrete parameters. By abuse of notation, and because simple multiplexes (with a unique input and a unique output) are replaced by a labeled arrow, resources can be either multiplexes or variables.

Parameter	Parameter	Parameter	Parameter
$\tilde{K}_{SK,\{\}} = 0$	$\tilde{K}_{B,\{\}} = 0$	$\tilde{K}_{A,\{\}} = 0$	$\tilde{K}_{En,\{\}} = 0$
$K_{SK,\{A\}} > 0$	$K_{B,\{A\}} \text{ ---}$	$K_{A,\{En\}} = 0$	$K_{En,\{A\}} = 0$
$K_{SK,\{SK\}} = 0$	$K_{B,\{m\}} \text{ ---}$	$K_{A,\{B\}} \text{ ---}$	$K_{En,\{SK\}} \text{ ---}$
$K_{SK,\{A,SK\}} = 2$	$K_{B,\{A,m\}} = 1$	$K_{A,\{SK\}} \text{ ---}$	$K_{En,\{EP\}} \text{ ---}$
		$K_{A,\{En,B\}} \text{ ---}$	$K_{En,\{A,SK\}} \text{ ---}$
	$K_{EP,\{\}} = 0$	$K_{A,\{En,SK\}} \text{ ---}$	$K_{En,\{A,EP\}} \text{ ---}$
	$K_{EP,\{B\}} = 1$	$K_{A,\{B,SK\}} \text{ ---}$	$K_{En,\{SK,EP\}} \text{ ---}$
		$K_{A,\{En,B,SK\}} = 1$	$K_{En,\{A,SK,EP\}} = 1$

assertion P (precondition) is satisfied before performing the program p and if the program terminates, then the assertion Q (postcondition) will be satisfied afterwards.” This constitutes *de facto* a specification of the program under the form of a triple, called Hoare triple.

Here, we view an experimental trace of the gene network as a program. The elementary instructions of this “program” are the observed transitions in the state graph of the gene network: An assignment of the form $x := x + 1$ or $x := x - 1$ corresponds to an actual observation at this time of the experiment, where the gene x has increased (which we note $x+$ for simplicity), or respectively decreased (which we note $x-$). Such an observation tells us that there is a transition somewhere in the state graph where gene x has changed its abstract expression level.

The first constraints are deduced from the classical behavior of the cell cycle: Its cyclic behavior starts from 00001, goes through a sequence of transitions and goes back to 00001. Both precondition and postcondition are then the constraints defining the state 00001. We have to determine the program corresponding to the sequence of transitions. Although the transitions between phases are known, the precise order of transitions inside a same phase is not. This leads us to consider 12 hypothetical sequences of transitions for the cell cycle. For lack of space, we consider only one of them leading to the following Hoare triple:

$$\left\{ \begin{array}{l} SK = 0 \\ EP = 0 \\ A = 0 \\ B = 0 \\ En = 1 \end{array} \right\} SK+; SK+; En-; A+; SK-; SK-;$$

$$B+; A-; EP+; En+; B-; EP- \left\{ \begin{array}{l} SK = 0 \\ EP = 0 \\ A = 0 \\ B = 0 \\ En = 1 \end{array} \right\}.$$

Using the genetically modified Hoare logic,²⁰ we obtained 13 exact values of parameters, and one inequality ($K_{SK,\{A\}} > 0$), see Table 1. Among the $3^4 \times 2^{22} = 339,738,624$ possible parameter valuations, only $2^{13} = 8192$ valuations satisfy the constraints.

Other constraints can be deduced from experimental timing properties, which cannot be used in the purely discrete modeling framework of Thomas. So, we switch to our enriched hybrid modeling framework to take benefit of time measures.

4.2. Determining celerities of hybrid models from temporal traces

According to Definition 4, there are 56 celerities. Among them, six celerities are useless because the resources and the state are incompatible: For instance $C_{SK,\{SK\},0}$ applies to states where $\eta(SK) = 0$ and SK is a resource of itself. However, when $\eta(SK) = 0$, SK cannot be a resource of itself. Moreover, the sign of many celerities is known from biological observations shown in Table 2 (the arrows give the sign of associated celerities).

In order to constrain celerities, we consider that the cell cycle phase durations are 10, 8, 4, and 0.5 h for phases G1, S, G2, and M.²¹ The time spent in each of qualitative states is approximated assuming that the duration of each phase is uniformly distributed in each of its states. This hypothesis will have consequences on the constraints on celerities. Adopting a reasoning way similar to the one of Sec. 4.1 (using Hoare logic on discrete models), we determine precisely five accurate points along the cell cycle: These five hybrid states allow us to deduce by Definition 6 relationships between time spent in some qualitative states and associated celerities.

In the sequel, we suppose that Boolean variables are attracted towards the external boundaries because this hypothesis does not change the reachability properties. Assuming this and according to Sec. 2.1, the discrete parameters allow the determination of the sign of the celerities (and conversely): If $K_{v,\omega} = 1$, then $C_{v,\omega,n} > 0$; If $K_{v,\omega} = 0$, then $C_{v,\omega,n} < 0$. Thus, we get the sign of six celerities leading to Table 3, which contains 38 constraints on celerities.

Table 2. Biological observations of the five variables during cell cycle. The first row represents the sequence of discrete states (see Sec. 4.1) crossed by the classical behavior of the cell cycle.

	00001	10001	20001	20000	20100	10100	00100	00110	00010	01010	01011	01001
	G1			S				G2		M		
SK	↗	↗	Max	Max	↘	↘	Min	Min	↗	↗	↗	↗
EP	Min	Min	Min	Min	Min	Min	Min	↗	↗	Max	Max	↘
A	Min	Min	Min	↗	↗	Max	Max	↘	↘	↘	Min	Min
B	Min	Min	Min	↗	↗	↗	↗	↗	Max	Max	↘	Min
En	Max	↘	↘	Min	Min	Min	Min	Min	↗	↗	Max	Max

Table 3. Constraints on celerities.

En	$C_{\text{En},\{\},0} < 0$	EP	$C_{\text{EP},\{\},0} < -\frac{3}{\Delta t_{G1}}$	
	$C_{\text{En},\{\},1} < 0$		$C_{\text{EP},\{\},1} = -\frac{3}{\Delta t_M}$	
	$C_{\text{En},\{A\},0} < -\frac{4}{\Delta t_S}$		$C_{\text{EP},\{B\},0} = \frac{1}{\Delta t_{G2}}$	
	$C_{\text{En},\{A\},1} = -\frac{3}{2*\Delta t_{G1}}$		$C_{\text{EP},\{B\},1} > \frac{3}{\Delta t_M}$	
	$C_{\text{En},\{\text{SK}\},0} < 0$		B	$C_{B,\{\},0} < -\frac{3}{\Delta t_M}$
	$C_{\text{En},\{\text{SK}\},1} < 0$			$C_{B,\{\},1} = -\frac{3}{\Delta t_M}$
	$C_{\text{En},\{A,\text{SK}\},0} < \frac{2}{\Delta t_{G2}}$			$C_{B,\{m\},0} < \frac{4}{\Delta t_S}$
	$C_{\text{En},\{A,\text{SK}\},1} > 0$			$C_{B,\{m\},1} > \frac{2}{\Delta t_{G2}} - C_{B,\{A,m\},1}$
$C_{\text{En},\{A,\text{EP},\text{SK}\},0} = \frac{6-3*\Delta t_{G2}*C_{\text{En},\{A,\text{SK}\},0}}{2*\Delta t_M}$	$C_{B,\{A,m\},0} = \frac{4-\Delta t_S*C_{B,\{m\},0}}{3*\Delta t_S}$	SK	$C_{B,\{A,m\},1} < \frac{2}{\Delta t_{G2}}$	
$C_{\text{En},\{A,\text{EP},\text{SK}\},1} > \frac{3}{\Delta t_M}$	$C_{\text{SK},\{\},0} < -\frac{4}{\Delta t_S}$			
A	$C_{A,\{\},0} < -\frac{6-(3*\Delta t_{G2}+2*\Delta t_M)* C_{A,\{\text{En}\},0} }{2*\Delta t_M}$		$C_{\text{SK},\{A\},0} = \frac{6}{2*\Delta t_{G1}+6*\Delta t_M+3*\Delta t_{G2}}$	
	$C_{A,\{\},1} < 0$		$C_{\text{SK},\{\text{SK}\},1} = -\frac{4}{\Delta t_S}$	
	$C_{A,\{B\},0} < 0$		$C_{\text{SK},\{\text{SK}\},2} = -\frac{4}{\Delta t_S}$	
	$C_{A,\{B\},1} < 0$		$C_{\text{SK},\{A,\text{SK}\},1} = \frac{3}{\Delta t_{G1}}$	
	$0 > C_{A,\{\text{En}\},0} > -\frac{2}{\Delta t_{G2}}$		$C_{\text{SK},\{A,\text{SK}\},2} > \frac{3}{\Delta t_{G1}}$	
	$C_{A,\{\text{En}\},1} = -\frac{2}{\Delta t_{G2}}$			
	$C_{A,\{B,\text{En}\},0} > 0$			
	$C_{A,\{B,\text{En}\},1} > \frac{4}{\Delta t_S} - C_{A,\{B,\text{En},\text{SK}\},1} > 0$			
	$C_{A,\{B,\text{SK}\},0} < 0$			
	$C_{A,\{B,\text{SK}\},1} < 0$			
	$C_{A,\{B,\text{En},\text{SK}\},0} = \frac{4}{\Delta t_S}$			
	$0 < C_{A,\{B,\text{En},\text{SK}\},1} < \frac{4}{\Delta t_S}$			

4.3. Additional biological observations

To determine parameters controlling behaviors outside of the classical cell cycle behavior, we have to take into account alternative observed trajectories, in particular about the quiescent phase and the endoreplication phenomenon.

- (1) We suppose $K_{B,\{A\}} = 0$ because EP and En inhibitors of B outweigh the activator A (A is ressource of B and m is not). Moreover, maintaining mitotic inhibitors involved in EP prevents the continuation of the cell cycle. Thus, it is assumed that the presence of EP keeps the activity of En: $K_{\text{En},\{\text{SK},\text{EP}\}} = K_{\text{En},\{A,\text{EP}\}} = K_{\text{En},\{\text{EP}\}} = 1$ (using also Snoussi's condition).
- (2) The endoreplication begins in mitosis and ends in G1 without going through cell division. Because endoreplication skips the first step of G1 and the duration of G1 is shortened,¹⁴ we deduce that the trajectory going from mitosis (skipping cell division) to the first step of G1 is forbidden, leading to the constraint $C_{A,\{\text{SK},\text{En}\},0} < 0$.
- (3) The quiescent phase is reachable from the end of mitosis. Because we can stay in G0 for a long time, the model has to present a cyclic behavior inside the G0

Table 4. Discrete parameters.

Parameter	Parameter	Parameter	Parameter
$K_{SK,\{\}} = 0$	$K_{B,\{\}} = 0$	$K_{A,\{\}} = 0$	$K_{En,\{\}} = 0$
$K_{SK,\{A\}} = 2$	$K_{B,\{A\}} = 0$	$K_{A,\{En\}} = 0$	$K_{En,\{A\}} = 0$
$K_{SK,\{SK\}} = 0$	$K_{B,\{m\}} = 1$	$K_{A,\{B\}} = 0$	$K_{En,\{SK\}} = 0$
$K_{SK,\{A,SK\}} = 2$	$K_{B,\{A,m\}} = 1$	$K_{A,\{SK\}} = 0$	$K_{En,\{EP\}} = 1$
		$K_{A,\{En,B\}} = 1$	$K_{En,\{A,SK\}} = 1$
	$K_{EP,\{\}} = 0$	$K_{A,\{En,SK\}} = 0$	$K_{En,\{A,EP\}} = 1$
	$K_{EP,\{B\}} = 1$	$K_{A,\{B,SK\}} = 0$	$K_{En,\{SK,EP\}} = 1$
		$K_{A,\{En,B,SK\}} = 1$	$K_{En,\{A,SK,EP\}} = 1$

phase. Among the two possible cyclic sequences of transitions inside G0 states, only one is compatible with previous constraints.

These remarks allowed us to find the set of useful celerities and the 26 discrete parameters of our model (see Table 4). Note that the discrete parameters do not make all regulations of Fig. 4 functional because the discretization is too rough to keep each regulation. At the opposite, each regulation is visible in terms of celerities.

5. Simulations

Several simulations were performed with parameters (celerities and initial states) picked to satisfy constraints of Sec. 4.2:

- Equality constraints give exact values of celerities.
- Inequality constraints lead to choices: For each constraint of the form $C < 0$ (respectively $C > 0$), we choose $C = -1$ (respectively $C = 1$). For each constraint of the form $0 < C < k$ (respectively $0 < k < C$) where k is a constant, we choose $C = 0.5 \times k$ (respectively $C = 1.5 \times k$). For negative celerities, we choose symmetrically their exact values by multiplying the constant of inequalities by 0.5 or 1.5.
- The chosen initial state is one of the hybrid states determined in Sec. 4.2.

Figure 5 shows the traces for such a simulation: After 22.5 h (simulated time), the simulation goes back exactly to the initial hybrid state from which the same behavior

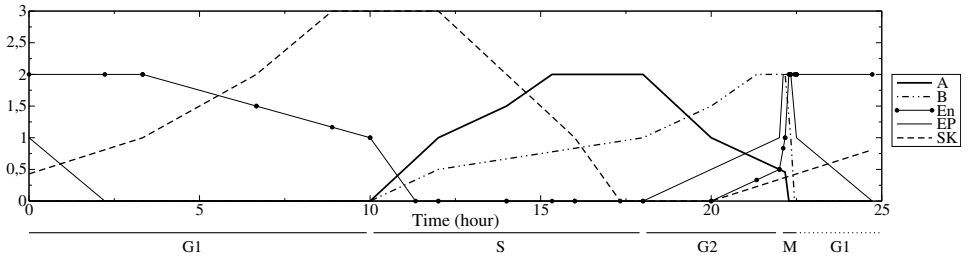


Fig. 5. A simulation representing the classical cell cycle behavior.

can be repeated infinitely. This cyclic behavior corresponds to the classical cell cycle trajectory. Moreover, it is a limit cycle because, when starting from a neighborhood of this cyclic trace, the limit cycle is reached again after a sufficient time.

Other simulations showed that endoreplication and remaining in the quiescent phase are also possible in the model (results not shown for lack of space).

6. Conclusion

We developed in this paper a hybrid formalism which is well suited for modeling time-dependent biological phenomena such as the mammalian cell cycle. Indeed, we built a model which exhibits the limit cycle representing the classical cell cycle, the endoreplication, and the quiescent phase. This has been made possible because of the wise choice of variables, in particular with the split of the cyclin complexes. The parameter choice was aided by the determination of constraints, but exact values rely on hypotheses (constants for exact values of celerities, equidistribution of time on all qualitative states within a phase). This model constitutes, to our knowledge, the first hybrid model of the cell cycle, which provides the proof of concept of our computer-aided method for parameter identification.

Our simulations did not allow us to observe traces remaining a long time in the quiescent phase, this constitutes the main limitation of our model. We have now to accurately tune the parameter values in order to get a model presenting such a trace but we did not find any parameter valuations satisfying this specification. If no valuation of parameters is compatible with a long stay in the quiescent phase, to improve our hybrid model, we could also make the hypothesis of a regulator which would modify the celerities during this phase.

Moreover, the model presented here is based on only one of the 12 possible sequences of transitions of the cell cycle (remember that the exact order of the sequence of transitions is not known). The next time-consuming task is now to take into account the other sequences which would lead to other possible parameter constraints and then to other hybrid traces. More generally, we have to handle a large set of possible sequences of transitions. Hopefully, this difficulty can be overstepped because our hybrid modeling framework can be assisted by computer-aided methods to determine the set of parameters. Thus, our ongoing work is also to develop an automation of the building of constraints on celerities and to study the predictability of our hybrid model.

Finally, a long term objective is to make a coupling of our cell cycle model with a model of the circadian clock,²² in order to apprehend the interactions between these cycles whose functioning plays an important role in oncology.²³

Acknowledgments

We are grateful to B. Miraglio and the different reviewers for their comments to improve the paper. This work is partially supported by the French National Agency

for Research (ANR-14-CE09-0011) and ANR “Investments for the Future” LABEX SIGNALIFE program (ANR-11-LABX-0028-01).

References

1. Thomas R, Boolean formalization of genetic control circuits, *J Theor Biol* **42**(3):563–585, 1973.
2. Thomas R, Kaufman M, Multistationarity, the basis of cell differentiation and memory. II, *Chaos* **11**(1):180–195, 2001.
3. Bernot G, Comet JP, Richard A, Guespin J, Application of formal methods to biological regulatory networks: Extending Thomas’ asynchronous logical approach with temporal logic, *J Theor Biol* **229**(3):339–347, 2004.
4. Corblin F, Fanchon E, Trilling L, Applications of a formal approach to decipher discrete genetic networks, *BMC Bioinformatics* **11**(1):385, 2010.
5. Bernot G, Sriram K, Képès F, Discrete delay model for the mammalian circadian clock, *ComplexUs* **3**:185–199, 2006.
6. Comet JP, Bernot G, Das A, Diener F, Massot C, Cessieux A, Simplified models for the mammalian circadian clock, *Procedia Comput Sci* **11**:127–138, 2012.
7. Comet JP, Fromentin J, Bernot G, Roux O, A formal model for gene regulatory networks with time delays, *Proc CSBio’2010*, Bangkok, Thailand, CCIS, Vol. 115, pp. 1–13, 2010.
8. Bernot G, Comet JP, Snoussi EH, Formal methods applied to gene network modelling, in *Logical Modeling of Biological Systems* (Wiley-ISTE, 2014), pp. 245–289.
9. Snoussi EH, Qualitative dynamics of piecewise-linear differential equations: A discrete mapping approach, *Dyn Stabil Syst* **4**:180–207, 1989.
10. Satyanarayana A, Kaldis P, Mammalian cell-cycle regulation: Several Cdks, numerous cyclins and diverse compensatory mechanisms, *Oncogene* **28**(33):2925–2939, 2009.
11. Gérard C, Goldbeter A, A skeleton model for the network of cyclin-dependent kinases driving the mammalian cell cycle, *Interf Focus* **1**:24–35, 2010.
12. Kohn KW, Molecular interaction map of the mammalian cell cycle control and DNA repair systems, *Mol Biol Cell* **10**(8):2703–2734, 1999.
13. Spencer S *et al.*, The proliferation-quiescence decision is controlled by a bifurcation in CDK2 activity at mitotic exit, *Cell* **155**(2):369–383, 2013.
14. Edgar BA, Orr-Weaver TL, Endoreplication cell cycles: More for less, *Cell* **105**(3):297–306, 2001.
15. Tyson JJ, Novak B, Temporal organization of the cell cycle, *Curr Biol* **18**(17):R759–R768, 2008.
16. Larochelle S *et al.*, Requirements for Cdk7 in the assembly of Cdk1/cyclin B and activation of Cdk2 revealed by chemical genetics in human cells, *Mol Cell* **25**(6):839–850, 2007.
17. Trunnell NB, Poon AC, Kim SY, Ferrell JE, Ultrasensitivity in the regulation of Cdc25C by Cdk1, *Mol Cell* **41**(3):263–274, 2011.
18. Kellogg DR, Wee1-dependent mechanisms required for coordination of cell growth and cell division, *J Cell Sci* **116**(24):4883–4890, 2003.
19. DePamphilis ML, de Renty CM, Ullah Z, Lee CY, The octet: Eight protein kinases that control mammalian DNA replication, *Front Physiol* **3**:368, 2012.
20. Bernot G, Comet JP, Khalis Z, Richard A, Roux O, A genetically modified Hoare logic, 2015, ArXiv: abs/1506.05887.
21. Feillet C *et al.*, Phase locking and multiple oscillating attractors for the coupled mammalian clock and cell cycle, *Proc Natl Acad Sci USA* **111**(27):9828–9833, 2014.

22. Muter J *et al.*, The clock protein period 2 synchronizes mitotic expansion and decidual transformation of human endometrial stromal cells, *FASEB J* **29**:13–14, 2015.
23. De Maria E, Fages F, Soliman S, On coupling models using model-checking: Effects of irinotecan injections on the mammalian cell cycle, in *Computational Methods in Systems Biology*, Springer, pp. 142–157, 2009.



Jonathan Behaegel is a Ph.D. student in computer science at the University of Nice-Sophia Antipolis in France since 2015 (September). He made a Master degree in Biology and in Bioinformatics at the Polytech'Nice engineering school where he got a multidisciplinary background. His research works focus on the hybrid modeling of the cell cycle and the circadian clock, and more particularly on their coupling. This pluridisciplinary research program implies both the Informatics lab (I3S, Sophia-Antipolis, France) and the Biology lab (iBV, Nice, France).



Jean-Paul Comet is a first class Full Professor in computer science at the École Polytechnique Universitaire of the University of Nice-Sophia Antipolis, France, since 2007. He was previously Assistant Professor at Genopole®-Evry from 2000 to 2007. After having completed his Ph.D. at the University of Compiègne from 1994 to 1998, he has been Post-doc in Bioinformatics at the Whitehead Institute/MIT Center for Genome Research in Cambridge (MA) in the United States. He supported his Habilitation at the University of Evry in 2006 and was recruited Professor in 2007. His research area is bioinformatics. He first worked on the biological sequence comparison and statistical analysis of comparison scores and on the analysis of microarray data. Since 2000 his research focuses on the formal modeling of complex biological systems in the context of genomics.



Gilles Bernot is exceptional class Full Professor in computer science at the École Polytechnique Universitaire of the University of Nice-Sophia Antipolis, France, since 2007. He was previously Full Professor at Genopole®-Evry from 1992 to 2007 and Assistant Professor at the Ecole Normale Supérieure of Paris (ENS Ulm) from 1987 to 1992. He obtained his Ph.D. at the university of Orsay in 1986 and Habilitation in 1992. His research area since 1999 is the formal modeling of biological complex systems in the context of genomics. Gilles Bernot has been founder and head of

the research team in formal methods for software engineering at the computer science laboratory of Evry from 1993 to 1999, director of the computer science laboratory of Evry from 1998 to 2004 (UMR CNRS), founder and head of the research team in bioinformatics from 2000 to 2005, founding codirector of the Epigenomics Project of Genopole® from 2003 to 2007 (deputy director since 2007), vice-president of the National Council of Universities (CNU) in computer science from 2003 to 2007 (approximately 3000 teaching researchers), Scientific Delegate at the French Agency for the Evaluation of Research (AERES, Life Sciences Dpt) from 2007 to 2009, founder and head of the research axis in bioinformatics of the MDSC pole (Discrete Modeling of Complex Systems, I3S laboratory at Sophia Antipolis) from 2007 to 2012.



Emilien Cornillon is a Ph.D. student in computer science applied to biology (I3S lab, Sophia-Antipolis, France) at the University of Nice Sophia-Antipolis, since September 2013. He made a Master degree in Bioinformatics where he got a multidisciplinary background. His research works focus on the formal reduction of gene networks and hybrid modeling of gene regulatory network with a special emphasis on the mammalian circadian clock.



Franck Delaunay received the M.Sc. and the Ph.D. degrees in biology from the University of Brest, France in 1988 and 1992, respectively. He then joined the University of Rennes, France (1992), the Karolinska Institute, Stockholm Sweden (1993) and the Ecole Normale Supérieure, Lyon, France (1998). Since 2000, he is Full Professor of animal physiology at the University of Nice, France. His research is performed at the Institute of Biology Valrose (CNRS/INSERM) where he leads a group working on chronobiology using molecular and cellular biology techniques, time lapse imaging, functional genomics and mouse genetics. His current research aims at using systems biology approaches in collaboration with modelers to understand the function and the dynamical behavior of the circadian clock and the cell cycle oscillators.